RSC Advances

PAPER

View Article Online
View Journal | View Issue

Cite this: *RSC Adv.*, 2017, **7**, 21815

An extended application of β-Ga_2O_3 single crystals to the laser field: Cr^{4+}:β-Ga_2O_3 utilized as a new promising saturable absorber

Wenxiang Mu,[a] Yanru Yin,[a] Zhitai Jia, *[ad] Lijuan Wang,[a] Jie Sun,[a] Mengxia Wang,[a] Cheng Tang,[a] Qiangqiang Hu,[a] Zeliang Gao,[a] Jian Zhang,[a] Na Lin,[a] Stefano Veronesi,[bc] Zhengping Wang,[a] Xian Zhao[a] and Xutang Tao *[a]

Received 15th February 2017
Accepted 6th April 2017

DOI: 10.1039/c7ra01905j

rsc.li/rsc-advances

Considering their easy growth and doping in bulk crystal growth, and good crystalline quality, β-Ga_2O_3 single crystals, a very important wide-bandgap semiconductor, are now also considered to be a promising optical crystal candidate. In this work, a Cr^{4+}:β-Ga_2O_3 single crystal has been grown successfully by the edge-defined film-fed growth method. The thermal conductivity of Cr^{4+}:β-Ga_2O_3 has been measured along the *a** direction at room temperature obtaining 16.2 W m^{-1} K^{-1}, and it was much larger than that of the usually used Cr^{4+}-doped crystals, such as $Y_3Al_5O_{12}$ (YAG) or YVO_4. The Raman spectrum indicated that the cutoff phonon energy of the β-Ga_2O_3 crystal was 767.8 cm^{-1}. A passively Q-switched nanosecond pulsed Nd:YAG laser based on a Cr^{4+}:β-Ga_2O_3 saturable absorber was experimentally demonstrated for the first time to our knowledge and its mechanism is explained by first-principles calculations. By inserting the Cr^{4+}:β-Ga_2O_3 crystal into the Nd:YAG laser cavity, a Q-switched laser operation was obtained with a maximum average output power of 50 mW. The corresponding pulse repetition rate, pulse width, and pulse energy were determined to be of 421.5 kHz, 235.2 ns and 0.12 μJ, respectively.

Introduction

Highly efficient ultra-fast lasers have attracted much attention in the fields of communication, material processing, medicine, *etc.*[1] Q-Switching is one of the most important and major techniques for generating short laser pulses on micro- and nano-second time scales. There are two types of Q-switching: active and passive ones. Compared with the active one, passive techniques can significantly simplify the operation, improve the compactness, reliability and efficiency, and reduce the cost of laser sources. The saturable absorber (SA) is the key element for a passive Q-switched laser. Many SAs have been studied such as color centers,[2] transition-metal ion doped crystals[3–5] and semiconductors.[6,7]

Transition-metal ions, in tetrahedral coordination, with $3d^N$ configuration are identified as a class of important active ions for SAs.[8,9] For example, many crystals such as Cr^{4+}:YAG,[4] V^{3+}:YAG,[10] Cr^{4+}:$Gd_3Ga_5O_{12}$,[11] Cr^{2+}:ZnS,[12] Co^{2+}:$LaMgAl_{11}O_{19}$ (ref. 13) have been extensively studied as SAs. Among these crystals YAG is a typical host crystal due to its favorable chemical and physical properties especially the good thermal conductivity and high damage threshold, which are beneficial for realizing high power laser output. So far the Cr^{4+}:YAG single crystal is the most common SA around 1 μm.[4] However, the maximum phonon energy of YAG (about 857 cm^{-1}) is relatively high, which is unfavorable for high power laser since it will easily lead to multi-phonon process.[14,15] Therefore, the exploration of new SA crystals with good physical properties, especially with high thermal conductivity and low phonon energy, has always attracted a lot of attention.[9]

β-Ga_2O_3 crystal is a sesquioxide which belongs to the monoclinic family (space group: *C*2/*m*). The gallium ions are located at tetrahedral and octahedral sites.[16] So far this host was at the center of a large research work, being an ultra wide-bandgap semiconductor.[17] Wide-bandgap materials are challenging in the field of high voltage field-effect transistors, Schottky barrier diodes and ultraviolet photoelectric devices.[18–21] The β-Ga_2O_3 crystal presents steady chemical and physical properties. Its thermal conductivity is about 27 W m^{-1} K^{-1} along *b* axes,[22] which is much larger than that of YAG (12.9 W m^{-1} K^{-1}).[23] This indicates that β-Ga_2O_3 crystal could be favorable as an SA for the laser pulses of high peak power and high repetition rate. On the other hand, in recent years, large size bulk β-Ga_2O_3 crystals have been grown by various melt-

[a]State Key Laboratory of Crystal Materials, Key Laboratory of Functional Crystal Materials and Device, Shandong University, Jinan, 250100, China. E-mail: z.jia@sdu.edu.cn; txt@sdu.edu.cn
[b]NEST Istituto di Nanoscienze CNR, Piazza S. Silvestro 12, I-56127 Pisa, Italy
[c]Dipartimento di Fisica, Università di Pisa, Largo B. Pontecorvo 3, I-56127 Pisa, Italy
[d]State Key Laboratory of Optoelectronic Materials and Technologies, Sun Yat-sen University, Guangzhou 510275, China

growth methods, for example: Czochralski method,[24] floating zone technique,[25] Bridgman method,[26] edge-defined film-fed growth (EFG) method[27] and so on. Therefore, the access of high quality and large-sized β-Ga_2O_3 crystals makes it possible to be applied in laser field. However, there is still no report on exploiting the capabilities of β-Ga_2O_3 crystal in laser field until now.

In this work, Cr^{4+}:β-Ga_2O_3 single crystal has been successfully grown by EFG method. The bivalent Mg^{2+} ion was co-doped into the crystal to increase the ratio of Cr^{4+}/Cr^{3+}. The thermal conductivity and maximum phonon energy have been measured. Moreover, the laser operation has been demonstrated with the SA of Cr^{4+}:β-Ga_2O_3 crystal and the mechanism of saturable absorption phenomenon is also explained by the first-principles calculation. We believe that this work may provide some reference for future research of β-Ga_2O_3 in laser.

Experimental section

Crystal growth

The Cr^{4+}:β-Ga_2O_3 single crystal was grown by using a RF-heating EFG furnace. Powder raw materials of β-Ga_2O_3 (purity 99.99%), MgO (purity 99.99%), Cr_2O_3 (purity 99.5%) were adequately mixed and pressed into tablets. The prepared tablets were loaded into the Ir crucible (Φ 60 × 60 mm^3) with an Ir die. The size of the die top and the width of the slit were 4 × 25 mm^2 and 0.5 mm, respectively. Then the materials were heated to the melting temperature of β-Ga_2O_3. The molten materials rose through the slit due to capillary action and spread over the top of the Ir die. A pure β-Ga_2O_3 seed crystal with ⟨010⟩ orientation was slowly moved down to touch the top surface of the die under a suitable temperature, at which the seed would neither melt nor expand significantly. After ten minutes stabilization, the seed was pulled up at a speed of 10 mm h^{-1}. The heating power was gradually adjusted to narrow the seed, namely necking. After the necking process, the pulling speed was gradually decreased to 6 mm h^{-1}. The temperature was also decreased in order to extend the crystal spreading out on the whole top section of the die. The crystal was grown under the atmosphere of 98% Ar, plus 2% O_2 in order to suppress the decomposition and evaporation of Ga_2O_3 at high temperature. After the growth, the crystal was cooled down to room temperature at a rate of 20–30 °C h^{-1}. To further increase the ratio of Cr^{4+}/Cr^{3+}, the crystal was annealed at 1400 °C for 50 h in air. The annealed (100)-faced sample used as an SA in the following laser operation is shown in Fig. 1.

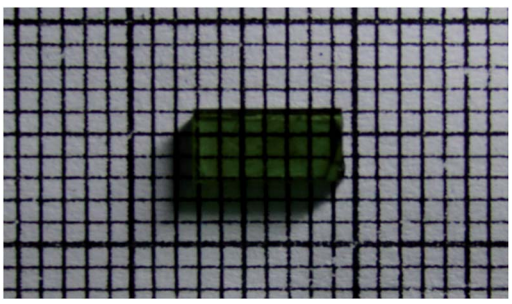

Fig. 1 Polished (100)-faced Cr^{4+}:β-Ga_2O_3 crystal sample after being annealed at 1400 °C for 50 h in air.

Thermal properties

The thermal conductivities of the Cr^{4+}:β-Ga_2O_3 and YAG crystals were measured using a Netzsch Nanoflash model LFA 457 apparatus by laser pulse method. The plate samples of 4 × 4 × 1 mm^3 in dimensions were cut from the bulk crystals. The larger faces were (100) plane for Cr^{4+}:β-Ga_2O_3, and (010) plane in the case of YAG. The samples coated with graphite on both square faces, were heated using a short light pulse over the temperature range of 25–700 °C. The specific heat was measured using a differential scanning calorimeter (Perkin-Elmer Diamond model DSC-ZC) over the temperature range of 20 °C to 300 °C with a heating rate of 5 °C min^{-1}. The accuracy of calorimetry and temperature for the instrument are less than 0.1% and ±0.01 °C, respectively. A sample weighing 90.3 mg was used during this measurement.

Raman spectroscopy and absorption spectrum

Room temperature Raman spectrum of β-Ga_2O_3 single crystal was measured by a Horiba Jobin Yvon LabRAM HR Raman spectrometer equipped with a Ge detector cooled by liquid N_2. A solid state laser at 633 nm with the power of 150 mW was used as excitation source. The absorption spectrum of Cr–Mg co-doped crystal grown by EFG method was measured by using a Varian Cary 500 spectrophotometer in the range of 190–1700 nm with a resolution of 1 nm.

Computational detail

In order to better understand the effect of Cr^{4+}-doping on β-Ga_2O_3 crystal, the first principles calculations were performed based on density functional theory with the projector-augmented wave (PAW) method, as implemented in the Vienna ab initio simulation package (VASP).[28] The generalized gradient approximation (GGA) functional of Perdew, Burke and Ernzerhof (PBE)[29] was used to approximate the exchange and correlation interactions. A cutoff energy of 400 eV for the plane-wave basis set and a Monkhorst–Pack mesh of 4 × 6 × 4 for the Brillouin zone integration were employed.

Pulse laser operation measurements

The laser experimental set-up is shown in Fig. 2. A simple concave-plano cavity was used to investigate the passive Q-switching Nd:YAG laser performance by using the Cr^{4+}:β-Ga_2O_3 single crystal as the SA. The pump source was an 808 nm fiber-coupled diode laser with a core diameter of 200 μm and a numerical aperture (N.A.) of 0.22. The pump beam was reimaged into the crystal by a 1 : 1 focusing system. M1 was a concave mirror with radius of curvature of 250 mm, which was anti-reflection (AR) coated at 808 nm on the entrance face, high-reflection (HR) coated at 1.06 μm and high-transmission (HT) coated at 808 nm on the other face. M2 was a flat mirror with transmission of 5% at 1.06 μm and HT coated at 808 nm. An

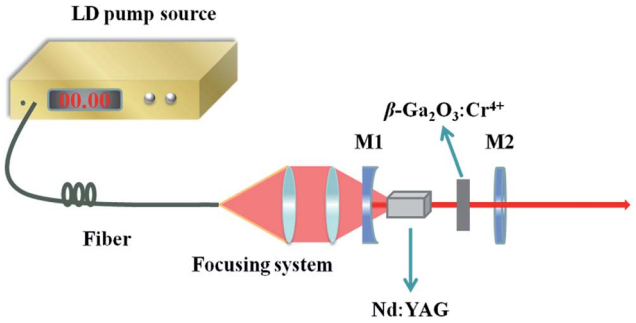

Fig. 2 Schematic diagram of the experimental laser setup.

uncoated and polished Nd:YAG crystal with dimensions of 4 × 4 × 7 mm^3 was used as the gain medium. In order to alleviate the thermal lensing effect, the Nd:YAG crystal was wrapped with an indium foil and mounted in a water-cooled copper holder maintained at a temperature of 16 °C. A polished (100)-faced Cr^{4+}:β-Ga_2O_3 crystal with the dimensions of 3 × 6 × 1 mm^3 was used as the SA without water cooling. The output power was measured by a power meter (POWERMAX 500D, Molectron Inc.), and the temporal behaviors of the Q-switched lasers were recorded by a 1 GHz bandwidth and 5.0 Gs per s sampling rate digital oscilloscope (DPO7104, Tektronix Inc.).

Result and discussion

Thermal properties

The thermal properties of crystals are crucial factors to be considered in high power laser. There are a little difference between the reported thermal conductivities of YAG (12.9, 10.7, 10.3, W m^{-1} K^{-1}).[23,30,31] Therefore, the conductivity of undoped YAG was also measured for comparison in our experiment. The thermal conductivities of Cr^{4+}:β-Ga_2O_3 and YAG crystals were shown in Fig. 3(a). As we can see, the thermal conductivity of Cr^{4+}:β-Ga_2O_3 along a^* is 16.2 W m^{-1} K^{-1} at room temperature, which is much larger than that of undoped YAG crystal of 11.7 W m^{-1} K^{-1}. Although the ion doping usually will induce lattice distortion of the crystals, and lead to a decrease of the thermal conductivity as a result. However, the thermal conductivity of Cr^{4+}:β-Ga_2O_3 is still much larger than that of undoped YAG crystal. What is more, the thermal conductivities along the b and c axes could be higher that of a^* axis according to previous research.[22] The higher thermal conductivity of Cr^{4+}:β-Ga_2O_3 will provide a better thermal management than of Cr^{4+}:YAG, which is quite essential especially to high power laser. The specific heat (C_p) of Cr^{4+}:β-Ga_2O_3 crystal as a function of temperature is shown in the Fig. 3(b). The C_p of Cr^{4+}:β-Ga_2O_3 increased almost linearly from 0.485 J g^{-1} K^{-1} at 20 °C to 0.747 J g^{-1} K^{-1} at 300 °C, comparable with the literature value of YAG (0.603 J g^{-1} K^{-1}).[23]

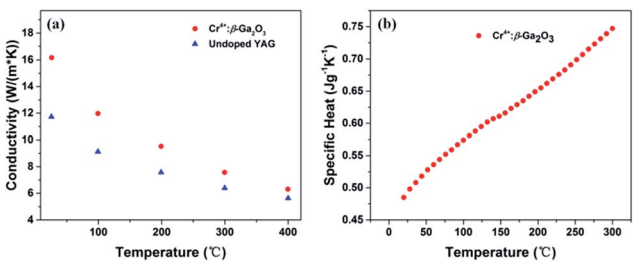

Fig. 3 (a) Thermal conductivities of Cr^{4+}:β-Ga_2O_3 and YAG, (b) specific heat of Cr^{4+}:β-Ga_2O_3 crystal.

Phonon energy

Host materials having low cutoff phonon energy will have a negligible multiphonon process behavior which is beneficial for enhancing the efficiency of laser operation. The phonon energy of laser host materials can be characterized by Raman spectra.[32] The Raman scattering spectrum of β-Ga_2O_3 single crystal was shown in Fig. 4. There are 11 peaks ranging from 100 cm^{-1} to 1000 cm^{-1}. The largest Raman shift peak was at 767.8 cm^{-1} which was in good agreement with the calculated value.[33] Therefore, the maximum phonon energy of β-Ga_2O_3 crystal is 767.8 cm^{-1}, which is lower than that of YAG (857 cm^{-1}).[14,15] This indicates that the β-Ga_2O_3 crystal should be a promising host material for laser applications.

Laser performance

Fig. 5(a) shows the relationship between the average output power and the absorbed pump power of the Q-switched laser. It shows a monotonously linear increase with augmenting the absorbed pump power. In order to protect the crystal from damage, the absorbed pump power was limited to 4.33 W and the maximum output power was 50 mW. No damage was observed on the crystals and mirrors in the laser experiment.

The pulse width and pulse repetition rate were recorded and they are shown in Fig. 5(b). By increasing the pump power, the pulse repetition rate increased from 290.5 to 421.5 kHz, while the pulse width shortened from 287 to 235.2 ns. The pulse trains and single pulse profile were shown in Fig. 6, which were obtained at

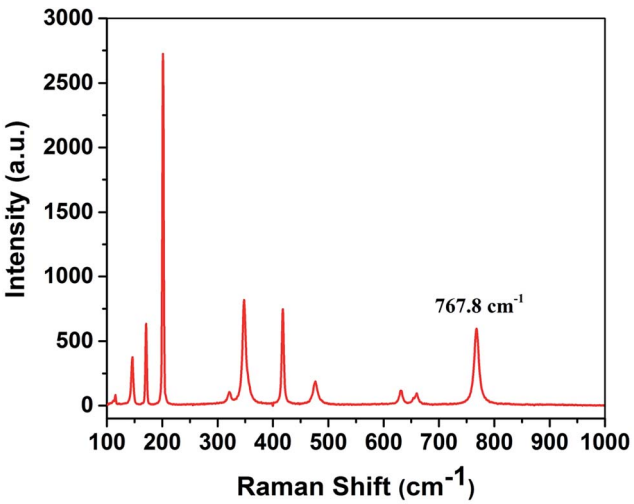

Fig. 4 Raman scattering spectrum of β-Ga_2O_3 single crystal.

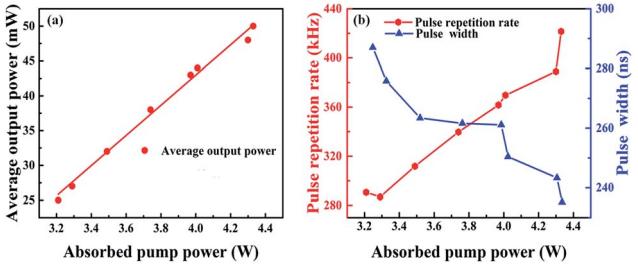

Fig. 5 (a) Average output power *versus* pump power for the Q-switching regime, (b) pulse width and pulse repetition frequency *versus* pump power.

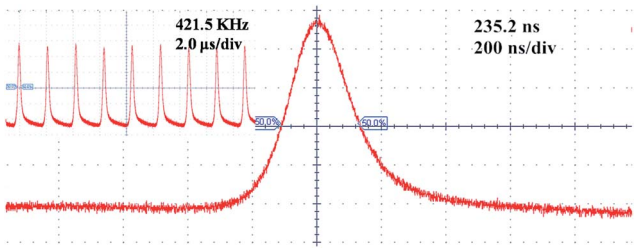

Fig. 6 The pulse train and single pulse profile at the maximum pump power of 4.33 W.

the maximum pump power of 4.33 W. At the maximum pump power the pulse duration and the corresponding pulse repetition rate were measured to be about 235.2 ns and 421.5 kHz, respectively. The maximum single pulse energy was calculated to be 0.12 μJ with a corresponding peak power of 0.51 W.

Mechanism of the saturable absorption

The calculated electronic and optical properties of pure and doped β-Ga_2O_3 are shown in Fig. 7(a). The electronic band gap of pure β-Ga_2O_3 is predicted to be 2.3 eV (Fig. 7(b)), which is consistent with previous calculated results,[34] however much smaller than the experimental results, (4.5–4.9) eV, due to the very well-known underestimation on band gap value of DFT-GGA. For Cr–Mg co-doped β-Ga_2O_3, the flat bands are found near the Fermi level in spin up states. Therefore, the band gap is largely decreased to 0.5 eV (Fig. 7(d)). From the partial density of states (PDOS), we note that the flat band states are mainly contributed by Cr atoms but little involved with Mg atoms. In addition, the decreased band gap is expected to be beneficial for long wavelength absorption of the doped β-Ga_2O_3 as excited by light. The optical properties are determined by the dielectric function $\varepsilon(\omega) = \varepsilon_1(\omega) + i\varepsilon_2(\omega)$, where the imaginary part $\varepsilon_2(\omega)$ can be obtained from the momentum matrix elements between the occupied and unoccupied wave functions, and the real part $\varepsilon_1(\omega)$ can be evaluated from $\varepsilon_2(\omega)$ using the Kramer–Kronig relations.[35] The absorption coefficient $\alpha(\omega)$ can be expressed as $\alpha(\omega) = \sqrt{2}\omega\left[\sqrt{\varepsilon_1^2(\omega) + \varepsilon_2^2(\omega)} - \varepsilon_1(\omega)\right]^{1/2}$, which is used to determine the absorption spectrum in the calculation. The measured absorption spectrum of Cr–Mg co-doped crystal

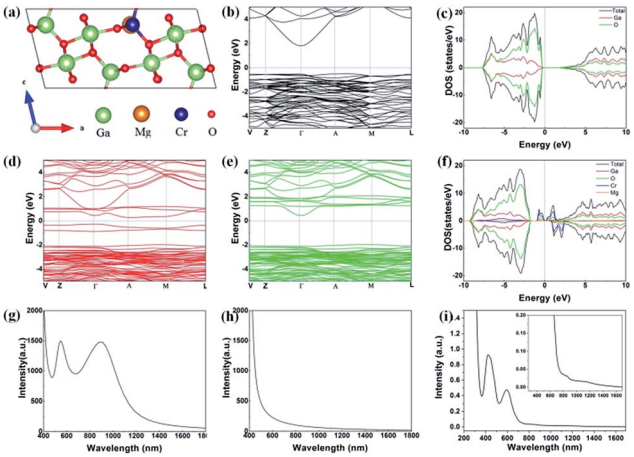

Fig. 7 (a) The optimized structure of Cr–Mg co-doped β-Ga_2O_3. The electronic band structure (b) and PDOS (c) of pure β-Ga_2O_3. Band structures of spin-up (d) and spin-down (e) electrons of Cr–Mg co-doped β-Ga_2O_3. (f) PDOS of Cr–Mg co-doped β-Ga_2O_3. Calculated absorption spectrum of pure (g) and Cr–Mg co-doped (h) β-Ga_2O_3. (i) The measured absorption spectrum of Cr–Mg co-doped crystal.

grown by EFG method was shown in the Fig. 7(i). For comparison, the calculated results are shown in Fig. 7(g) and (h). From Fig. 7(g) we can see that there is no obvious absorption peak of pure β-Ga_2O_3 in the region of wavelength lager than 600 nm apart from the intrinsic absorption peak located at ~440 nm. Nevertheless, two distinct absorption peaks individually located at 600 and 1000 nm appear in Cr–Mg co-doped β-Ga_2O_3, which correspond to the electrons transition from the doping states. When doped β-Ga_2O_3 is under strong excitation, the final states may be fully occupied and exhibited saturable absorption. This is also the reason that the experiment observed saturable absorption of Cr–Mg co-doped β-Ga_2O_3 at 1064 nm.

Conclusions and prospect

In this work, the β-Ga_2O_3 crystal has been studied and successfully demonstrated as a laser element for the first time. The Cr^{4+}-doped β-Ga_2O_3 crystal has been grown by EFG method. Passively Q-switched laser based on Cr^{4+}:β-Ga_2O_3 SA was experimentally demonstrated. Cr^{4+}:β-Ga_2O_3 has high thermal conductivity (16.2 W m^{-1} K^{-1}) and favorable maximum phonon energy (767 cm^{-1}). We obtained a Q-switched laser operation with a maximum average output power of 50 mW, a pulse repetition rate of 421.5 kHz, a pulse width of 235.2 ns and a pulse energy of about 0.12 μJ was demonstrated. In conclusion, considering the easy large-scale fabrication of crystal, good thermal properties and low phonon energy, the β-Ga_2O_3 crystal should be a promising laser element crystal, not only used as SAs after doping with Cr or Co transition-metal ions but also as laser crystal, doped with Ti ions in the future.

Acknowledgements

We gratefully acknowledge the financial support from the National Natural Science Foundation of China (Grant No.

51321091, 51227002, 51272129, 51323002), the National key Research and Development Program of China (Grant No. 2016YFB1102201), the Young Scholars Program of Shandong University (Grant No. 2015WLJH36), and the Program of Introducing Talents of Disciplines to Universities in China (Grant No. b06015).

Notes and references

1 U. Keller, *Nature*, 2003, **424**, 831–838.
2 J. A. Morris and C. R. Pollock, *Opt. Lett.*, 1990, **15**, 440–442.
3 A. Agnesi, A. Guandalini, G. Reali, J. K. Jabczynski, K. Kopczynski and Z. Mierczyk, *Opt. Commun.*, 2001, **194**, 429–433.
4 Y. Shimony, Z. Burshtein, A. B. A. Baranga, Y. Kalisky and M. Strauss, *IEEE J. Quantum Electron.*, 1996, **32**, 305–310.
5 K. V. Yumashev, *Appl. Opt.*, 1999, **38**, 6343–6346.
6 Y. Tsou, E. Garmire, W. Chen, M. Birnbaum and R. Asthana, *Opt. Lett.*, 1993, **18**, 1514–1516.
7 E. I. Ismail, N. A. Kadir, A. A. Latiff, H. Ahmad and S. W. Harun, *RSC Adv.*, 2016, **6**, 72692–72697.
8 S. Kück, *Appl. Phys. B*, 2001, **72**, 515–562.
9 Y. Kalisky, *Prog. Quantum Electron.*, 2004, **28**, 249–303.
10 A. Malyarevich, I. Denisov, K. Yumashev, V. Mikhailov, R. Conroy and B. Sinclair, *Appl. Phys. B*, 1998, **67**, 555–558.
11 Y. Wang, Z. Jia, X. Su, B. Zhang, R. Zhao, X. Tao and J. He, *Opt. Mater. Express*, 2016, **6**, 2600–2606.
12 H. Yu, V. Petrov, U. Griebner, D. Parisi, S. Veronesi and M. Tonelli, *Opt. Lett.*, 2012, **37**, 2544–2546.
13 K. Yumashev, I. Denisov, N. Posnov, N. Kuleshov and R. Moncorge, *J. Alloys Compd.*, 2002, **341**, 366–370.
14 J.-J. Song, P. B. Klein, R. L. Wadsack, M. Selders, S. Mroczkowski and R. K. Chang, *J. Opt. Soc. Am.*, 1973, **63**, 1135–1140.
15 V. Petrov, K. Petermann, U. Griebner, V. Peters, J. Liu, M. Rico, P. Klopp and G. Huber, *Proc. SPIE*, 2006, 62160H.
16 S. Geller, *J. Chem. Phys.*, 1960, **33**, 676–684.
17 D. Gogova, M. Schmidbauer and A. Kwasniewski, *CrystEngComm*, 2015, **17**, 6744–6752.
18 S. Fujita, *Jpn. J. Appl. Phys.*, 2015, **54**(3), 836–845.
19 M. Higashiwaki, K. Sasaki, A. Kuramata, T. Masui and S. Yamakoshi, *Phys. Status Solidi A*, 2014, **211**, 21–26.
20 P. Song, Z. Wu, X. Shen, J. Kang, Z. Fang and T.-Y. Zhang, *CrystEngComm*, 2017, **19**, 625–631.
21 K. Kachel, M. Korytov, D. Gogova, Z. Galazka, M. Albrecht, R. Zwierz, D. Siche, S. Golka, A. Kwasniewski, M. Schmidbauer and R. Fornari, *CrystEngComm*, 2012, **14**, 8536–8540.
22 Z. Guo, A. Verma, X. Wu, F. Sun, A. Hickman, T. Masui, A. Kuramata, M. Higashiwaki, D. Jena and T. Luo, *Appl. Phys. Lett.*, 2015, **106**, 111909.
23 K. Y. Kuwano, K. Suda, N. Ishizawa and T. Yamada, *J. Cryst. Growth*, 2004, **260**, 159–165.
24 Z. Galazka, K. Irmscher, R. Uecker, R. Bertram, M. Pietsch, A. Kwasniewski, M. Naumann, T. Schulz, R. Schewski, D. Klimm and M. Bickermann, *J. Cryst. Growth*, 2014, **404**, 184–191.
25 E. G. Víllora, K. Shimamura, Y. Yoshikawa, K. Aoki and N. Ichinose, *J. Cryst. Growth*, 2004, **270**, 420–426.
26 K. Hoshikawa, E. Ohba, T. Kobayashi, J. Yanagisawa, C. Miyagawa and Y. Nakamura, *J. Cryst. Growth*, 2016, **447**, 36–41.
27 A. Hideo, N. Kengo, T. Hidetoshi, A. Natsuko, S. Kazuhiko and Y. Yoichi, *Jpn. J. Appl. Phys.*, 2008, **47**, 8506–8509.
28 J. P. Perdew, K. Burke and M. Ernzerhof, *Phys. Rev. Lett.*, 1996, **77**, 3865–3868.
29 M. Brandbyge, J.-L. Mozos, P. Ordejón, J. Taylor and K. Stokbro, *Phys. Rev. B: Condens. Matter Mater. Phys.*, 2002, **65**, 165401.
30 S. Chénais, F. Druon, F. Balembois, P. Georges, A. Brenier and G. Boulon, *Opt. Mater.*, 2003, **22**, 99–106.
31 A. Slack and D. W. Oliver, *Phys. Rev. B: Condens. Matter Mater. Phys.*, 1971, **4**, 592–609.
32 H. Guo, N. Dong, M. Yin, W. Zhang, L. Lou and S. Xia, *J. Phys. Chem. B*, 2004, **108**, 19205–19209.
33 B. Liu, M. Gu and X. Liu, *Appl. Phys. Lett.*, 2007, **91**, 172102.
34 T. C. Lovejoy, R. Chen, E. N. Yitamben, V. Shutthanadan, S. M. Heald, E. G. Villora, K. Shimamura, S. Zheng, S. T. Dunham and F. S. Ohuchi, *J. Appl. Phys.*, 2012, **111**, 123716–123716.
35 P. Y. Yu and M. Cardona, *Fundamentals of Semiconductors: Physics and Materials Properties*, Springer, Berlin, Heidelberg, 1996.